Astron. Astrophys. 329, 991–1009 (1998)

ASTRONOMY
AND
ASTROPHYSICS

The nature of OH/IR stars in the galactic centre

J.A.D.L. Blommaert[1,2,3], **W.E.C.J. van der Veen**[4], **H.J. Van Langevelde**[5], **H.J. Habing**[1], **and L.O. Sjouwerman**[6]

[1] Sterrewacht Leiden, P.O. Box 9513, 2300 RA Leiden, The Netherlands
[2] ISO Science Operations Centre, Astrophysics Division, Space Science Dept. of ESA, Villafranca, P.O. Box 50727, E-28080 Madrid, Spain
[3] CNRS, Institut d'Astrophysique de Paris, 98bis, Blvd Arago, F-75014 Paris, France
[4] Columbia University, Dept. Of Astronomy, 538 West 120th Street, New York, NY 10027, USA
[5] Joint Institute for VLBI in Europe, P.O. Box 2, 7990 AA Dwingeloo, The Netherlands
[6] Onsala Space Observatory, S-439 92 Onsala, Sweden

Received 22 January 1997 / Accepted 5 August 1997

Abstract. We report on infrared observations of stars in a field of 30′ near the galactic centre. All these objects were previously detected as OH (1612 MHz) maser sources. For a large fraction of these stars variability data are available from a VLA monitor programme. This makes it possible to correct the IR measurements for variability. Corrections for interstellar extinction are also applied. The resulting infrared colours, periods and luminosities are compared with results for other samples of OH/IR stars and it is shown that the galactic centre stars are similar to the same type of objects in the bulge of the Galaxy but that more luminous (and thus younger) stars exist in the centre. The question of the existence of two distinct populations of OH/IR stars near the galactic centre is addressed, but the limited number of stars inhibits a firm conclusion. We do find that when the sample is divided according to OH expansion velocity, the dust-to-gas mass loss ratio, which depends on metallicity, is on average twice as high for the high expansion velocity group as for the low expansion velocity stars. The luminosities and the number density of the low expansion velocity stars are consistent with them being an extension of the bulge population, whereas the high expansion velocity group contains brighter sources and is more likely to be a population intrinsic to the galactic centre. The previously proposed period-luminosity (PL-) relation for OH/IR stars can be studied with this sample. We find that the OH/IR stars significantly deviate from the PL-relation and argue that the OH/IR stars have evolved away from the PL-relation. It was found that non-variable OH/IR stars are often associated with peculiar IR sources.

Key words: stars: AGB and post – AGB – stars: evolution – Galaxy: center – infrared: stars

1. Introduction

At the galactic centre the stellar density, ρ, reaches a maximum. This cannot be inferred from visual observations which suffer from very high visual extinction. The maximum was first observed at 2 μm (Becklin and Neugebauer 1968). The 2 μm surface brightness profile indicates that ρ follows an $r^{-1.8}$ dependence and Becklin and Neugebauer estimated that in the inner 1 pc ρ is about 10^7 times its value near the sun and within 100 pc the average stellar density is probably 10^3 higher than in the solar neighbourhood. This picture has changed little since 1968 (see Sellgren 1989 or Genzel et al. 1994 for a review). The more than 100 OH/IR stars discovered by Lindqvist et al. (1992a) are roughly consistent with this estimate of ρ.

The large density of OH/IR stars observed towards the galactic centre also indicates that they are physically at the galactic centre. This is confirmed by their kinematics based on radial velocities derived from the OH(1612 MHz) lines. Although peculiar stellar motions at the galactic centre are quite high ($\approx$ 100 km/s), a net rotation of the stars is clearly seen around a centre that coincides with the postulated location of the centre of the Galaxy (Lindqvist et al. 1992b). In the rest of this paper we will assume that the OH/IR stars discussed here are all at the same distance of R_0 = 8 kpc (e.g., Reid 1993 and references therein).

The masers from these OH/IR stars are probably the only stellar features at the galactic centre that are not affected by interstellar extinction. Even at 2μm it is not easy to study the stellar content of the inner 100 pc. The mean visual extinction is about 25 magnitudes and appears to be quite patchy, resulting in about 2.2 mags of extinction at 2μm. Fortunately at longer wavelengths, where OH/IR stars emit most of their energy, the extinction is less allowing us to study these stars both in the IR and in the OH maser line.

1.1. OH/IR stars

When low and intermediate mass stars approach the end of their lives they go through a relatively short phase lasting about $10^5 - 10^6$ yr which is known as the the Asymptotic Giant Branch (AGB) phase. Miras, carbon stars and OH/IR stars are all examples of AGB stars. Miras and OH/IR stars are characterized by

Send offprint requests to: J. Blommaert (Villafranca, Spain)

long-period pulsations (P= 200-2000 days) with bolometric amplitudes up to 1 mag and high mass loss rates ($> 10^{-7} M_{\odot}/yr$). The mass loss creates circumstellar shells that redden the underlying red giant and give rise to several other phenomena, such as OH masers (see Habing 1996, for a review on AGB stars).

OH/IR stars are among the most extreme oxygen-rich AGB stars. They have the longest periods (P $\gtrsim$ 500 days) and the highest mass loss ($\dot{M} > 10^{-5} M_{\odot}/yr$). The high mass loss speeds up the AGB evolution by depleting the stellar envelope on a time scale of $\approx 10^4$ yr. The mass loss also dominates the appearance of the star. The circumstellar shell totally obscures the underlying red giant star, and the shell itself is detectable as a strong infrared source at wavelengths around 10 μm, where the stellar luminosity is reemitted by the cool dust shell. In the shell several types of masers may be present depending on the physical conditions in the shell. Most often the OH maser at 1612 MHz is the strongest of these masers (see Cohen 1989 or Elitzur 1992, for a review on masers).

As Miras and OH/IR stars share many characteristics it has been suggested that they are closely related. In colour-colour diagrams, especially those based on IRAS data, these two types of objects form a continuous sequence (van der Veen and Habing 1988). The Miras, which are optically visible, are less red than OH/IR stars, which have the highest mass loss. One possible interpretation is that the sequence is purely evolutionary: Miras ultimately evolve into OH/IR stars. A second possibility is that stellar mass uniquely parameterizes this sequence: more massive stars evolve into OH/IR stars, less massive stars into Miras. A third possibility is a combination of both where at least some evolution takes place but where initial mass also plays a role. Studying these stars in different locations within our galaxy may help us choose between these possibilities.

One informative parameter of OH/IR stars, which is very easy to measure and distance independent is the expansion velocity of the OH shell. It is measured directly from the OH profile as half the separation between the blue and red-shifted peak. Baud et al. 1981 showed that the expansion velocity is systematically larger for population I OH/IR stars, e.g. those at low galactic latitudes. Because the final outflow velocity is determined by radiation pressure on dust in the circumstellar shell, it is expected that both the total luminosity and the metallicity of the star play a role in determining the expansion velocity (e.g. Schutte and Tielens, 1989 and Habing et al. 1994).

1.2. OH/IR stars in the inner Galaxy

Near the galactic centre we find a large sample of about 200 OH/IR stars, all at about the same relatively well known distance. This sample is well suited to study AGB evolution without being affected by large uncertainties in distances. At the same time, although not independently, one can study these objects to learn about the stellar content of the inner 100 pc.

In a survey for OH 1612 MHz masers with the VLA, 134 OH/IR stars were detected in the central 100 pc (Lindqvist et al. 1992a). Recently, Sjouwerman et al. (1996) have added about 50 stars within 50 parsec of the galactic centre as a result of a more sensitive search. The main goal of the Lindqvist et al. survey was to study stellar velocities in the galactic centre region (Lindqvist et al. 1992b). The kinematical behaviour of this sample seems to indicate that different populations of OH/IR stars may be involved: stars with high expansion velocities seem to rotate in a flatter system than those with low expansion velocities.

In Van Langevelde et al. (1993) (hereafter VJGHW) a subsample of these objects was monitored in OH using the VLA and yielded accurate periods for 13 stars. Most periods are shorter than 800 days, a result similar as found for OH/IR stars in the galactic bulge based on IR variability data (Whitelock et al. 1991 and van der Veen and Habing 1997). The absence of periods well over 1000 days is in contrast with the presence of such long pulsation periods found for OH/IR stars in the galactic disk (Herman and Habing 1985, Engels et al. 1983, Van Langevelde et al. 1990). In this paper we will determine the bolometric luminosities of galactic centre OH/IR stars and compare them with those found for bulge stars. We will also compare the period-luminosity relations for Miras and OH/IR stars, that were proposed by Whitelock et al. (1991) and Feast et al. (1989).

2. Observations

2.1. Sample

We selected 34 OH maser sources: 31 from the Lindqvist et al. (1992a) sample and three "high-velocity" OH/IR stars (Baud et al. 1975, van Langevelde et al. 1992a). The selected OH masers are roughly within a $28' \times 28'$ area. Twenty-four of these OH masers were monitored for OH variability (VJGHW). For 12 OH masers the light curve analysis yielded a unique period; for seven sources no unambiguous period could be determined. Five OH masers did not show a well-behaved light curve.

We included mostly OH masers for which a variability study was done in order to correct the bolometric magnitudes for variability.

2.2. Observing runs

The sample of 32 OH masers was observed in 1990, 1991 and 1993 with the ESO 2.2 m and 3.6 m at La Silla (Chile) and the 3.8 m United Kingdom Infrared Telescope (UKIRT) at Mauna Kea (Hawaii). In Table 1 the observing dates, telescopes and instruments are listed.

For all sources we have accurate VLA positions ($\sim 0.2''$) which facilitated their identification. Observations were made using IR cameras at the shortest wavelengths (up to 4μm) and traditional single-channel photometers.

2.2.1. The 1990 season

During our first run in June 1990 at ESO, IRAC camera observations were conducted in the H (1.65 μm) and K (2.2 μm) band with the ESO 2.2 m telescope. Originally K and L (3.8 μm) measurements were planned, but because of problems with the 64 $\times$ 64 pixels array (Hg:Cd:Te/CCD) we had to use a 32 $\times$ 32 array of the same type but with a cutoff at 3.4 μm. These

Table 1. Log of the observing runs; absence of an entry for diaphragm in column 4 indicates IR array imaging

Run	Telescope	Dates	Diaph. [$''$]	Wavelength Range [μm]	Instruments
1	ESO 2.2	5/6/90		1.65 - 2.20	IRAC
2	ESO 3.6	12-13/6/90	5	2.20 - 4.66	InSb
3	UKIRT 3.8	30/6/90	6	2.20 - 4.66	UKT9
4	UKIRT 3.8	10/8/90	5	3.75 - 20.0	UKT8
5	ESO 2.2	24/6/91		2.20 - 3.80	IRAC
6	ESO 2.2	30/6/91 - 1/7/91	5	2.20 - 12.9	InSb/Bolometer
7	UKIRT 3.8	6-10/8/91		2.20 - 3.45	IRCAM
8	UKIRT 3.8	27-28/8/91	5	2.20 - 20.0	IRCAM/UKT8
9	UKIRT 3.8	17-19/6/93	5	1.25 - 4.65	IRCAM/UKT9
10	UKIRT 3.8	3/7/93	5	3.8 - 20.0	UKT8

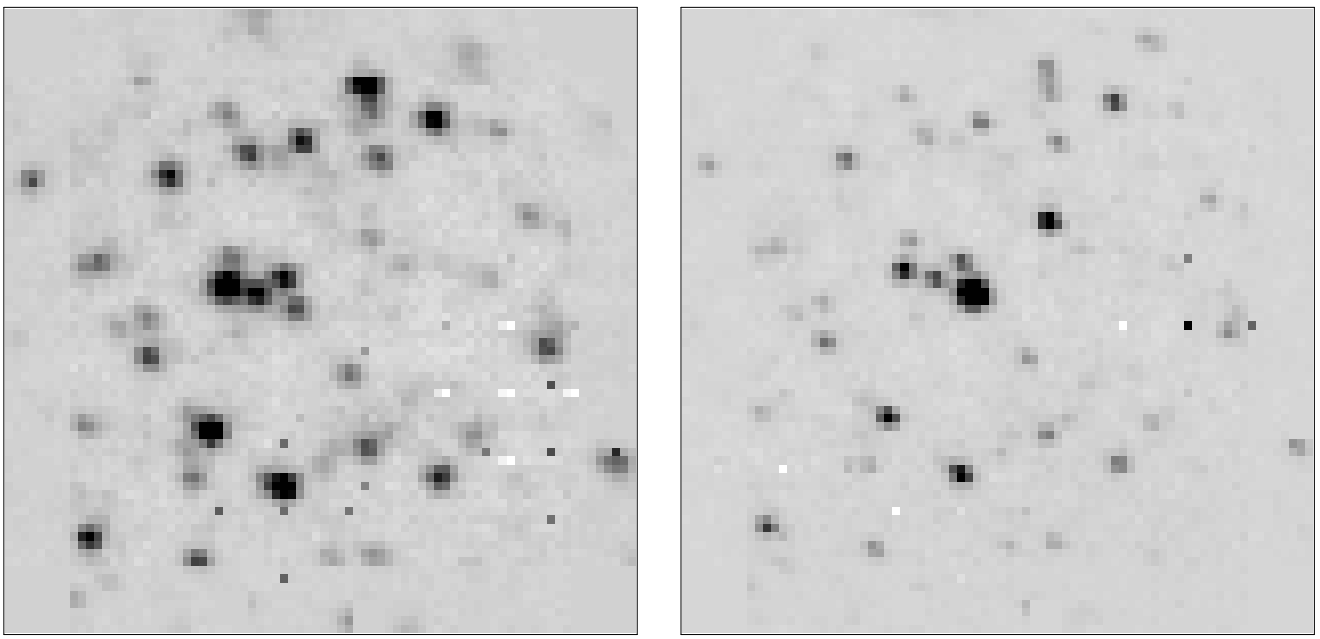

Fig. 1. K and nbL band images of OH0.178-0.055 taken with the IRCAM camera. These figures show the threat of confusion and illustrates the necessity of camera work at the shorter wavelengths ($\lambda < 4\mu m$) to make an unambiguous identification. The program source is identified with the source near the centre of the image that stands out in the nbL image (right).

measurements did not yield sufficient photometric accuracy and were only used as finding charts for the single channel photometry at the 3.6 m ESO telescope a week later.

Each aperture photometry observation was preceded by centering on a nearby bright star. After this the programme source was searched for in the L band. Standard chopping and beamswitching techniques were used with an aperture of $5''$ at the 3.6 m. Such a small aperture was used to reduce the probability of having more than one source in the beam. This is still important at the K-band, but considerably less important at the longer wavelength L (3.8 μm)- and M (4.7 μm) bands. Because of the high number of sources in this field one also has to be careful that the reference beam is actually measuring empty sky. For this reason the IRAC images were used to find a clean beamswitching direction. The observing conditions were only moderately good during a small part of the time and for only five sources useful data between 2.2 to 4.8 μm was obtained (Table 2).

On June 30 and August 10, 1990 another 9 sources were measured between 2 and 20 μm using the UKT8 and UKT9 instruments on UKIRT under photometric conditions.

2.2.2. The 1991 and 1993 season

In 1991 a new IRAC array was installed at ESO thus allowing L-band measurements. The camera was used in K and L to overcome possible confusion. These measurements were then combined with single channel photometry between 2.2 and 12.5 μm.

Table 2. Observed magnitudes for the galactic centre OH sources. Subsequent rows list the magnitudes and errors respectively. Column 2-5 UKIRT and ESO short wavelength bands, 6-9 ESO (N1, N2 and N3) and UKIRT (8.4, 9.6, 12.5 μm and Q) bands. Lower limits for the magnitudes are preceded by "$>$"-sign. Dashes indicate non-detections. The last column refers to Table 1.

Name	K	nbL	L	M	N1	N2	N3	Q	Obs. run
OH359.675+0.069	9.56	6.56							9
	0.05	0.03							
OH359.678-0.024					4.19	5.00	3.10	2.15	4
					0.07	0.20	0.12	0.14	
	7.81	5.50							8
	0.01	0.05							
	8.05	5.59	5.00	4.19					9
	0.05	0.03	0.01	0.01					
OH359.755+0.061	9.49	7.82							7
	0.02	0.12							
	9.30	8.18							9
	0.02	0.02							
			8.25	7.37					
			0.05	0.06					
OH359.762+0.120	8.18		3.96	3.04	1.34	1.95	0.11	-0.66	3,4
	0.01		0.01	0.02	0.03	0.05	0.04	0.02	
	9.85		5.17						5
	0.04		0.03						
OH359.776-0.120			9.68	8.28	6.30	6.30	5.20		4
			0.06	0.17	0.30	0.40	0.40		
	$>$20.3	10.57							7
		0.15							
	14.09	10.97	8.66	6.98					9
	0.06	0.04	0.02	0.08					
OH359.799-0.090	11.53		6.60	5.87	4.31	$>$ 9.50	2.82	2.71	3,4
	0.02		0.02	0.03	0.09		0.10	0.16	
	12.09	8.58							7
	0.04	0.11							
OH359.810-0.070					4.34	6.10	3.43		4
					0.13	0.80	0.11		
	8.79	6.26							7
	0.04	0.05							
	9.39	6.83	6.66	6.10					9
	0.05	0.03	0.04	0.04					
OH359.825-0.024	9.81		5.88	4.93	3.45	4.7	2.6		6
	0.02		0.05	0.04	0.10	0.4	0.2		
	9.61	6.41							7
	0.03	0.11							

The 62 $\times$ 58 IRCAM array at UKIRT was used to measure K and narrow-band nbL (3.45 μm) magnitudes for 21 sources. The selected pixel scale was 0.6″. Single-channel photometry between 3.8 and 20 μm was done on August 28, 1991. The same procedure was used in 1993 for 21 sources which were measured between 2.2 and 20 μm. For a couple of peculiar objects (Sect. 4.3) we used IRCAM to also measure the J and H-bands.

2.3. Data reduction

The aperture photometry was reduced in the usual way using standard star measurements to estimate the extinction. The IRAC and IRCAM frames were reduced in a standard way using the ESO-MIDAS software and the AIPS software respectively. The magnitudes derived are listed in Table 2.

For clarity, we mention that in the further analysis the (small) differences between the ESO and UKIRT K and M (2.2 and

Table 2. (continued)

Name	K	nbL	L	M	N1	N2	N3	Q	Obs.run
OH359.837+0.120	11.76	7.92	6.97	5.78	-	-	-		9,10
	0.02	0.03	0.01	0.02					
OH359.880-0.087	18.67	14.48							9
	0.36	0.36							
OH359.906-0.041	12.10	9.28							7
	0.05	0.11							
	12.56	8.65	7.26	6.31					9
	0.05	0.03	0.02	0.02					
			7.26	6.31					
OH359.918-0.056	7.97	6.01	5.44	4.83	5.01	5.37	3.89	1.79	9,10
	0.02	0.02	0.01	0.01	0.12	0.28	0.24	0.10	
OH359.938-0.077			9.60		7.10	8.80	5.40	3.90	4
			0.30		0.40	1.60	0.50	0.50	
	-	-	10.46	9.45					9
			0.04	0.38					
OH359.943+0.260	8.20		5.00	4.19					6
	0.06		0.05	0.04					
	8.49	5.69			2.96	3.74	1.87	0.83	8
	0.02	0.12			0.03	0.12	0.05	0.09	
	8.77	5.76							9
	0.05	0.03							
OH359.952-0.036	-		-	-					5,6
					-	-	-		8
	-	-							9
OH359.954-0.041	10.67	7.45							7
	0.07	0.11							
		8.02	6.67	5.31	5.97	6.80	3.27	1.99	9,10
		0.02	0.01	0.02	0.25	0.76	0.12	0.12	
OH359.971-0.119	15.7		7.25	5.07	2.70	6.2	1.21		6
	0.4		0.04	0.05	0.08	1.6	0.10		
	$>$ 14.20	8.95							7
		0.12							
OH359.974+0.162	$>$ 14.60	8.33							7
		0.11							
	12.11	8.09	7.00	5.73					9
	0.05	0.03	0.01	0.01					
OH359.977-0.087	$>$ 17.06	11.7	8.73	5.99	4.35	6.79	3.25	3.74	9,10
		0.09	0.02	0.02	0.08	0.87	0.14	0.55	

4.7 μm) and between the ESO L and UKIRT L' (3.8 μm) have been ignored. When the L-band is used in for instance a colour determination it refers to the 3.8 μm wavelength band and *not* to the nbL-band (3.45 μm).

Despite the high source densities we are confident about the final identification of the target sources. We used very accurate VLA positions ($\approx$0.2$''$) and the pointing of the UKIRT telescope was excellent so that the sources were always exactly in the centre of the IRCAM image. An example of the high source density in these galactic centre fields is illustrated in Fig. 1 which shows the K and nbL IRCAM image of OH0.178-0.055.

In Fig. 2 a diagram of the [3.8]-[4.7] colour versus [2.2]-[3.8] colour is shown for our sample. The colours are corrected for interstellar extinction in the manner that will be discussed

Table 2. (continued)

Name	K	nbL	L	M	N1	N2	N3	Q	Obs.run
OH0.040-0.056	9.70		5.81	4.98					3
	0.02		0.02	0.02					
	10.81		6.60	5.66					6
	0.04		0.09	0.06					
	10.50	7.11			4.33	6.03	2.78	2.24	8
	0.05	0.05			0.10	0.76	0.10	0.36	
OH0.060-0.018	10.41		6.26	5.36	4.1	5.3	2.9		5,6
	0.07		0.06	0.04	0.2	0.8	0.3		
	9.91	7.00							7
	0.01	0.05							
OH0.071-0.205	13.78		7.90	5.09					2
	0.76		0.36	0.83					
					3.68	6.10	2.31	1.62	4
					0.05	0.30	0.06	0.08	
OH0.071+0.127	12.46		6.64	5.27	3.48				6
	0.03		0.06	0.04	0.12				
	12.18	7.35			3.47	4.70	2.33	1.48	8
	0.08	0.05			0.04	0.34	0.08	0.22	
OH0.076+0.146	10.63		6.47	5.50	3.62	5.4	2.6		6
	0.02		0.06	0.05	0.11	0.7	0.2		
	10.75	7.58							7
	0.04	0.05							
OH0.079-0.114			6.95	5.29					2
			0.18	0.06					
			8.43	6.44					6
			0.04	0.05					
	14.76	9.95							7
	0.41	0.14							
	14.56	9.57	8.85	6.95					9
	0.03	0.04	0.02	0.03					
OH0.113-0.060	12.53	9.72							7
	0.06	0.13							
	12.80	8.58	7.28	5.50					9
	0.02	0.04	0.01	0.01					
OH0.129+0.103	8.44		6.11	5.60	4.4				5,6
	0.04		0.05	0.04	0.4				
					0.08	0.27	0.10	0.18	
					4.69	5.21	3.17	1.37	8

in the next section. In the same diagram an IRAS selected sample of galactic bulge OH/IR stars (van der Veen and Habing 1990) is shown (these colours are not corrected for interstellar correction as this correction is small ($E(K-L) \lesssim 0.1$ and $E(L-M) \lesssim 0.03$). Both groups occupy the same region in the diagram confirming our expectation that the galactic centre OH masers are true OH/IR stars and further confirming that our identifications in the crowded near IR frames are correct.

3. Determination of mean bolometric magnitudes

To convert the observed magnitudes at various wavelengths to mean bolometric magnitudes corrections were made for interstellar extinction and source variability. The followed procedure is explained below. In the calculations we have neglected the small differences between the ESO and UKIRT filter system and have adopted the central wavelengths and fluxes for a 0 mag star of the ESO system for both the ESO and UKIRT data. We estimate that this results in an error of only 0.005 mag in the

Table 2. (continued)

Name	K	nbL	L	M	N1	N2	N3	Q	Obs.run
OH0.142+0.026	9.55		5.59	4.63					2
	0.14		0.19	0.06					
			4.93		3.04	3.87	1.78	0.96	4
			0.02		0.04	0.08	0.06	0.08	
	9.92	6.68							7
	0.02	0.10							
	9.94	6.89	6.04	4.98					9
	0.02	0.02	0.01	0.02					
OH0.178-0.055			5.91	4.70	3.30	5.00	2.26		6
			0.03	0.04	0.09	0.50	0.16		
	11.25	6.88							7
	0.06	0.05							
OH0.189+0.052	11.82		5.89	4.56	2.78	4.6	1.84		5,6
	0.09		0.06	0.04	0.06	0.4	0.12		
	11.91	7.28							7
	0.05	0.05							
OH0.190+0.036	11.68		6.92	5.58					2
	0.14		0.19	0.06					
	11.44		6.50	5.14	3.39	4.7	2.31		6
	0.02		0.06	0.04	0.09	0.4	0.16		
	11.42	7.27							7
	0.03	0.11							
OH0.225-0.055	11.00		7.06	5.70					2
	0.17		0.22	0.08					
	10.16	6.93	6.13	5.18	3.67	4.76	2.47	2.01	9,10
	0.02	0.03	0.01	0.01	0.07	0.16	0.08	0.15	
OH0.319-0.040	-	-							9
OH0.334-0.181a	12.8	11.70							9
	0.02	0.05							
OH0.334-0.181b	9.81	7.76	7.15	6.83					9
	0.02	0.03	0.01	0.05					

final bolometric magnitudes derived from UKIRT observations, i.e. very small compared to other error contributions discussed below. We have not used the UKIRT nbL magnitudes.

3.1. Extinction correction

The IR observations of the GC OH/IR stars must be corrected for interstellar extinction. The extinction correction at a given wavelength λ, A_λ, is usually given as a fraction of the visual extinction, A_λ/A_V, and a universal galactic extinction curve is assumed. Catchpole et al. (1990) published a map of A_V towards the galactic centre region based on J, H and K measurements. They show that the visual extinction (A_V) globally varies from 20 to 30 magnitudes, but is also quite patchy. Regions with much higher extinction values of A_V up to 60 mag and more are known to exist in the galactic centre region (Glass et al. 1996). These regions are small and the chance that our stars coincide with such dark clouds is small. As no quantitative information on the position and the extinction of these clouds is available at this time we adopt an average value of $A_V = 25 \pm 2$ mag for all GC OH/IR stars. This 1 σ error takes only the global variation of 20 to 30 magnitudes A_V into acount.

We have considered two extinction laws often used in the literature: (1) as given by Rieke and Lebofsky (1985) and (2) the standard curve no. 15 of van de Hulst (1949). When we use the Rieke and Lebofsky extinction law the dereddened spectral energy distributions of the OH/IR stars look distorted, showing a bump at $3.8\mu m$ (L-band), see Fig. 3 for a typical example. The problem is not solved by assuming A_V that varies from source to source and appears to be caused by the adopted extinction law.

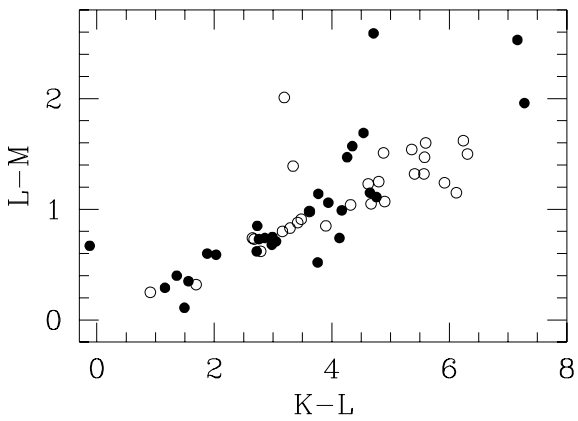

Fig. 2. Colour-colour diagram to check the identifications as OH/IR stars. The closed symbols indicate sources in the current sample and have been corrected for interstellar extinction (see Sect. 3.1). Open symbols are measurements of galactic bulge OH/IR stars by van der Veen and Habing (1990), not corrected for extinction ($E(K-L) \lesssim 0.1$ and $E(L-M) \lesssim 0.03$).

Table 3. The adopted extinctions for different wavelengths. The extinction values in the 2-5μm part are derived by using the standard curve no. 15 of van de Hulst (1949). Between 8 and 13μm Rieke and Lebofsky (1985) is used to correct for the interstellar extinction feature.

$\lambda(\mu$ m)	V	2.2	3.8	4.7	8.4	9.7	12.9
A_λ	25.0	2.14	1.05	0.83	0.90	2.20	0.70

The distortion does not occur when using curve no. 15 of van de Hulst (1949). Unfortunately this curve has no correction for the interstellar 9.7 μm silicate feature and because OH/IR stars have a circumstellar silicate feature of their own one cannot correct the spectral energy distribution (SED) by simply removing the silicate feature. Okuda et al. (1990) obtained satisfactory results for stars in the galactic centre region by correcting the interstellar silicate feature using the Rieke and Lebofsky extinction law between 8 and 13μm and $A_{\rm V}$ = 25 and this procedure we therefore adopted. In Table 3 the adopted extinction values and the different wavelengths at which they were applied are given.

In summary, we use the standard curve no. 15 of van de Hulst (1949) to correct the 2-5μm part of the SED for interstellar extinction and we use the Rieke and Lebofsky (1985) law at longer wavelengths up to 13μm. An example of a SED that was corrected for interstellar extinction is shown in Fig. 3.

3.2. Bolometric magnitudes

After interstellar extinction corrections we have determined bolometric magnitudes. This required an extrapolation to longer wavelengths. Our measurements at best yield the total flux between 2 and 13μm by integrating under the observed SED. To determine the bolometric magnitudes we use two bolometric corrections, $m_{\rm bol} = m_{\rm NIR} + BC_{\rm NIR}$ and $m_{\rm bol} = L_o + BC_{\rm L}$ (see Appendix A). Here $m_{\rm NIR}$ is the near IR magnitude corresponding to the total observed flux between 2 and 13μm, $\rm L_o$ is the 3.8μm magnitude and both $\rm BC_L$ and $\rm BC_{NIR}$ are a function of $\rm (L\text{-}M)_o$ colour.

We now distinguish two cases. The best case is to have photometry over the entire 2.2-12.9μm wavelength range (20 sources). We then calculate $m_{\rm NIR}$ by integrating F_ν as function of ν and using the trapezium integrating rule by connecting the F_ν values by straight lines. This works very well, after a small correction (see Appendix A) this integration technique introduces an error of only about 0.04 mag. The total error in $m_{\rm NIR}$ however may be larger due to the errors in the individual magnitudes used for the integration. To give some idea of this error we found that if all magnitudes between 2.2 and 12.9μm had the same error of 0.05 mag the resulting error in $m_{\rm NIR}$ would only be 0.02 mag which would combine with the 0.04 mag error due to the integration technique to a total error of 0.06 mag. The values of $m_{\rm NIR}$ are then converted to $m_{\rm bol}$ using the appropriate bolometric correction from the Appendix A. Combining all error contributions including the error due to a possible spread in $\rm A_V$ of $\pm$2 mag and due to the bolometric correction, which have errors given in the Appendix A, we find that the final error in the bolometric magnitudes is typically 0.1 mag.

The second case is when we have only 2.2-4.7μm data (eight sources). We now use only the $\rm L_o$ magnitudes and the $\rm (L\text{-}M)_o$ colour to determine $m_{\rm bol}$ using the appropriate bolometric correction from the Appendix A. The combined error due to all error contributions is larger because errors in the $\rm L_o$ magnitudes and $\rm (L\text{-}M)_o$ colours carry a large weight. We find that a typical error in the bolometric magnitudes determined this way is 0.2 mag, substantially larger than where we have data for the entire 2.2-12.9μm spectrum.

3.3. Variability correction

Finally the bolometric magnitudes are corrected for variability to determine the mean bolometric magnitudes. These corrections are not negligible and peak to peak variations of the bolometric magnitudes of 1-2 mag have been observed (e.g. van der Veen and Habing 1990).

To make the variability correction we use mostly results of the OH monitoring programme (VJGHW). It has been well established that the OH luminosity and IR luminosity vary simultaneously (e.g. Harvey et al. 1974, Engels et al. 1983). We follow Herman and Habing (1985) and VJGHW in describing the variability as

$$M_{\rm bol}(t_i) =< M_{\rm bol} > -\Delta M \cos\left(2\pi\phi(t_i)\right), \qquad (1)$$

where

$$\phi(t) = \begin{cases} \frac{\varphi}{2f} & \text{when } 0 \le \varphi < f, \\ \frac{\varphi-1}{2(1-f)} + 1 & \text{when } f \le \varphi \le 1, \end{cases}$$

and

$$\varphi = (t_i - t_0)/P.$$

The mean bolometric magnitudes are calculated using the pulsation periods, times of maximum light and light curve asymmetry factors (f) from VJGHW. Herman et al. (1984) adopt that

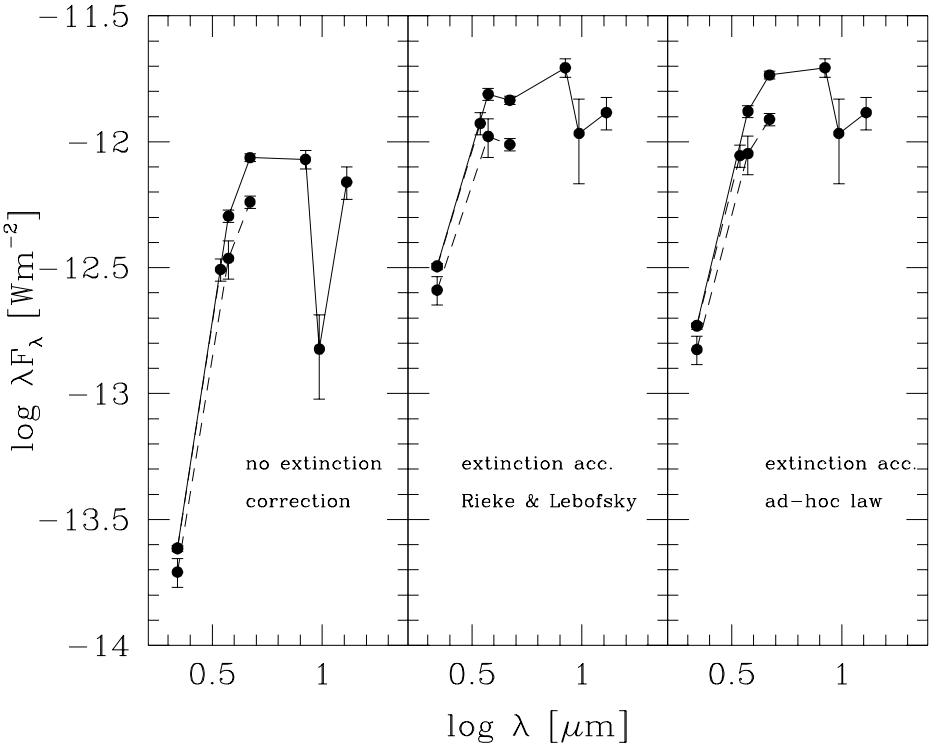

Fig. 3. Energy distributions for OH0.190+0.036 (three measurements at different epochs are indicated). Left: raw data before extinction correction. Middle: corrected with the Rieke and Lebofsky (1985) curve. Right: extinction correction with our ad-hoc approach.

the amplitude in the bolometric luminosity is twice the amplitude in the radio on measured ratios for 6 OH/IR stars. Note that VJGHW define b as the amplitude in $\log(F)$ and not in $2.5\log(F)$.

For four sources for which no periods were reported by VJGHW we have used periods determined by Jones et al. (1994) from the L band photometry. In this case we have used the mean OH amplitude (b = 0.13, Table 3 of VJGHW) to calculate the bolometric amplitude (0.65 mag). Further we assumed f = 0.5 ± 0.05 and the times of maximum were determined from the published light curves as they are not tabulated by Jones et al. (1994)

The variability correction was determined for 22 sources. Depending on the phase of the light curve at the time of the IR observations the correction and the error in it covers a large range of values being smallest at phases 0.25 and 0.75 and largest at phases 0 and 0.5. The final mean bolometric magnitudes and the errors are listed in Table 5; the errors are typically 0.2 to 0.5 mag. Table 5 also list the bolometric magnitudes and errors before the variability correction and $M_{\rm bol}$ assuming a distance modulus of 14.51 corresponding to a distance of 8 kpc.

Table 4 lists several parameters for the sources in our sample. The period, the expansion velocity of the shell, the amplitude of the OH variability and the mean OH flux are taken from Lindqvist et al. (1992a) and from VJGHW. If a source did not show evidence for variability this is indicated by a dashed line (group 3 in VJGHW). Underlined periods indicate variable sources for which no period could be determined unambiguously (group 2 in VJGHW). The period entry was left blank when sources are not in the monitor samples of VJGHW or Jones et al. (1994). When periods were taken from Jones et al. (1994) this is indicated in the last column.

3.3.1. Comments on individual sources

Six sources need extra mention in addition to the results of the Tables 2 and 5:

- OH359.755+0.061 The IRCAM source in the centre has a blue K-nbL colour. With UKT8 a red source was picked up and measured in L and M. The latter magnitudes have been used to derive the bolometric magnitude in Table 5. The derived bolometric magnitude is less certain as the $BC_{\rm L}$ (Appendix A) applied may not be relevant as the source has possibly an energy distribution different from a normal OH/IR star (see the discussion on this source in Sect. 4.4.)
- OH359.810-0.070 As the association of the near-infrared measurement with the 10 μm observation was doubtful, the identification was considered uncertain and not used in further analysis.
- OH359.918-0.056 Relatively blue colours in the near-infrared. The source has an excess at 20 μm which may explain the presence of an OH maser for this relatively blue source.
- OH359.938-0.077 has $M_{\rm bol}$ = -0.9. This value is more uncertain as this source may not be a genuine AGB-type OH/IR star (see Sect. 4.4) which means that the bolometric correction applied (Appendix A) would not be relevant.
- OH0.319-0.040 Not detected.
- OH0.334-0.181 At the position of the radio source only a weak blue object was found (object a in Table 2). One

Table 4. Parameters for the sample of OH/IR stars. Periods are taken from VJGHW or Jones et al. 1994, a dashed line indicates "no variability" according to VJGHW. ΔV is the separation of the OH peaks (VJGHW and Lindqvist et al. 1992a), $b_{\rm OH}$ is the amplitude of the OH variations (VJGHW), $F_{\rm OH}$ is the flux density of the brightest OH peak (VJGHW and Lindqvist et al. 1992a). Blanks indicate parameters that were not observed. In the last column it is indicated when the period was taken from Jones et al. 1994 (J) or when the sources are high velocity sources (HV) (Van Langevelde et al. 1992a)

Name	P [days]	ΔV [km/s]	$b_{\rm OH}$	$F_{\rm OH}$ [Jy]	*Comm.*
OH359.678-0.024	645	43.2		0.31	J
OH359.755+0.061	- - -	37.5	- - -	0.60	
OH359.762+0.120	758	29.6	0.18	5.75	
OH359.776-0.120	404	26.1	0.12	0.62	
OH359.799-0.090	625	36.8	0.13	1.32	
OH359.825-0.024	644	42.0	0.10	0.63	
OH359.837+0.120		38.0		0.38	HV
OH359.906-0.041	700	39.7		0.56	J
OH359.918-0.056		38.0		0.87	HV
OH359.938-0.077	- - -	24.8	- - -	7.08	
OH359.943+0.260		34.0		0.48	
OH359.954-0.041	781	40.8	0.14	3.02	
OH359.971-0.119	1391	38.7	0.13	0.53	
OH359.974+0.162	712	47.8	0.12	0.30	
OH359.977-0.087	1070	33.6	0.13	0.78	
OH0.040-0.056	670	41.7		0.53	J
OH0.060-0.018	470	39.7	0.13	0.83	
OH0.071-0.205	752	27.3	0.14	2.09	
OH0.071+0.127	475	36.4	0.12	0.33	
OH0.076+0.146	639	41.9	0.11	0.78	
OH0.079-0.114	700	29.6		0.83	J
OH0.113-0.060	1135	34.2	0.12	0.58	
OH0.129+0.103	480	22.8	0.13	1.32	
OH0.142+0.026	734	46.3	0.15	1.00	
OH0.178-0.055	551	32.3	0.14	0.93	
OH0.189+0.052	843	39.7	0.13	0.76	
OH0.190+0.036	541	28.4	0.12	2.51	
OH0.225-0.055	- - -	32.9	- - -	2.51	

redder object (b) was detected but its position is 20" away from the OH maser source. We do not believe the second object is related to the OH maser source because of the large difference position and its very blue colour (the bluest in our sample). For this reason the source was not included in Table 5 and in our further analysis.

3.4. Comparison with $M_{\rm bol}$ of Jones et al. (1994)

Jones et al. (1994) have monitored several stars of the Lindqvist et al. (1992a) sample in the L band. In their paper they show that the periods are generally in good agreement with the results of the OH monitoring by VJGHW. On basis of the L-band light curves and a single measurement in the K and M band Jones et al. derive bolometric magnitudes. We have 12 objects in common and a comparison between the bolometric magnitudes determined by us and by Jones et al. is shown in Fig. 4. On average the bolometric magnitudes of Jones et al. are 0.5 mag brighter.

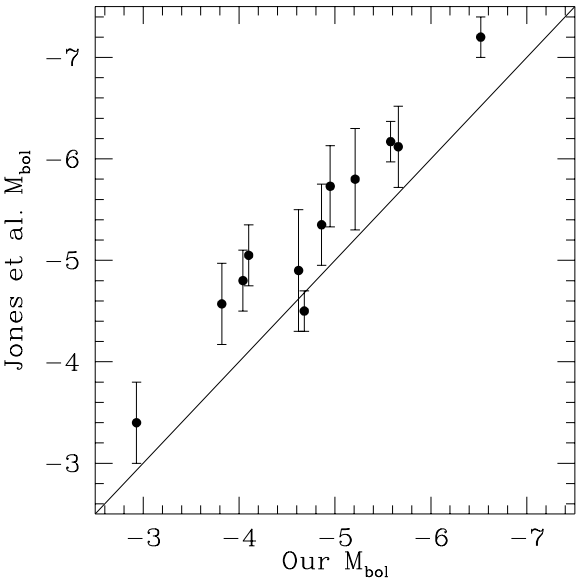

Fig. 4. A comparison of the bolometric magnitudes of GC stars as derived in this paper and by Jones et al. (1994). The error bars indicate the 1σ uncertainties in our bolometric magnitude derivation. The Jones et al. magnitudes are on average 0.5 mag brighter.

This difference is not due to differences in the photometry. Jones et al. (1994) have used the L-magnitude observed by us in two of their light curves and they find good agreement. We confirm that the photometry by Jones et al. agrees well with our photometry for all twelve sources we have in common. We believe, however, that the systematic difference noted above is due to the use of a different bolometric correction for L-band. Jones et al. use a bolometric correction (BC_L versus L-M colour) which is different from ours by about 0.5 mag. This bolometric correction for the 3.8 μm L-band was adapted from a bolometric correction determined for the 3.5 μm L-band by Jones et al. 1982 using photometry between 1 and 10 or 20 μm. We believe that our correction is more reliable for two reasons. First, we have determined the bolometric correction for the L-band actually used in our paper. Second, we have determined the bolometric corrections using photometry between 2 and 60 μm which provides a much better coverage of the SED of OH/IR stars (see Appendix A).

4. Discussion

4.1. Comparison with other samples

The infrared colours of the OH/IR stars are indicative of the dust optical depths in their circumstellar shells and are thus a measure of their dust mass loss rates. We have chosen the K-L

Table 5. The average $M_{\rm bol}$ and $\sigma(M_{\rm bol})$ are determined as described in Sect. 3. Underlined values for $M_{\rm bol}$ are not corrected for variability. In column 4 or 5 either the $L_o$magnitude or the near IR magnitude are given, depending which one was used to determine $M_{\rm bol}$. The corresponding bolometric correction is given in column 7. In column 6 the $(L-M)_o$ colour used to determine the BC is given. In the last columns the phase of the observation and the determined variability correction are given (see formula 1).

Name	$M_{\rm bol}$	$\sigma(M_{\rm bol})$	L_o	m_{NIR}	$(L-M)_o$	BC	$\varphi(t_i)$	$\Delta M\cos(2\pi\phi(t_i))$
OH359.678-0.024	-5.6	0.3	3.95		0.58	4.50	0.11	0.49
OH359.755+0.061	<u>-2.9</u>	0.2	7.20		0.65	4.41	- -	- -
OH359.762+0.120	-6.5	0.2		7.61	0.69	-0.32	0.90	0.71
OH359.776-0.120	-2.9	0.4	7.61		1.46	3.43	0.91	0.54
OH359.799-0.090	-4.0	0.3		10.56	0.50	-0.26	0.77	0.17
OH359.825-0.024	-5.2	0.5		9.67	0.73	-0.33	0.74	-0.03
OH359.837+0.120	<u>-4.6</u>	0.2	5.92		0.96	4.03	- -	- -
OH359.906-0.041	-3.8	0.4	6.21		0.73	4.33	0.79	0.16
OH359.918-0.056	<u>-5.2</u>	0.1		9.53	0.38	-0.21	- -	- -
OH359.938-0.077	<u>-0.9</u>	0.5	9.41		0.79	4.25	- -	- -
OH359.943+0.260	<u>-5.9</u>	0.1		8.86	0.58	-0.28	- -	- -
OH359.954-0.041	-4.1	0.3		10.69	1.13	-0.48	0.81	0.26
OH359.971-0.119	-6.0	1.0		9.64	1.96	-0.76	0.26	-0.38
OH359.974+0.162	-4.4	1.1	5.95		1.04	3.94	0.24	0.22
OH359.977-0.087	-3.7	0.2		11.11	2.52	-0.96	0.04	0.64
OH0.040-0.056	-4.9	0.4	4.76		0.61	4.47	0.14	0.42
OH0.060-0.018	-4.1	0.1		10.15	0.68	-0.32	0.02	0.63
OH0.071-0.205	-4.6	0.5		10.31	2.59	-0.98	0.11	0.57
OH0.071+0.127	-4.5	0.3	5.59		1.14	3.81	0.98	0.61
OH0.076+0.146	-5.0	0.4		10.11	0.75	-0.34	0.32	-0.21
OH0.079-0.114	-4.1	0.3	7.80		1.67	3.17	0.40	-0.53
OH0.113-0.060	-4.7	0.7	6.23		1.55	3.31	0.17	0.26
OH0.129+0.103	-4.0	0.1		10.02	0.28	-0.18	0.01	0.66
OH0.142+0.026	-5.7	0.4		9.27	0.74	-0.34	0.73	-0.08
OH0.178-0.055	-4.7	0.2		9.63	0.99	-0.42	0.91	0.59
OH0.189+0.052	-5.1	0.9		9.36	1.11	-0.47	0.06	0.54
OH0.190+0.036	-4.7	0.2		9.91	1.13	-0.48	0.87	0.41
OH0.225-0.055	<u>-5.0</u>	0.1		9.88	0.73	-0.33	- -	- -

colour because they are also available for two other relevant samples we want to compare our sample with.

The first comparison sample contains IRAS selected sources in two narrow strips in the direction of the galactic bulge ($7^\circ < |b| < 8^\circ, 345^\circ < l < 15^\circ$) with IRAS flux density ratios F_{25}/F_{12} between 0.7 and 2.0 (Whitelock et al. 1991). Whitelock et al. concluded based on IR photometry and a long-term monitoring program that these sources are predominantly AGB stars showing long-period variability and undergoing large mass loss (up to $3\times10^{-5}M_\odot/yr$). Part of this sample has also been observed in the OH(1612 MHz) maser line (te Lintel Hekkert et al. 1991) and 26% was detected.

The second comparison sample (van der Veen & Habing 1990) contains 37 IRAS sources in the direction of the galactic bulge and selected from region IIIb in the IRAS two-colour diagram (van der Veen & Habing 1988) which contains mostly AGB stars with very thick shells. Region IIIb corresponds to IRAS flux density ratios F_{25}/F_{12} between 1.2 and 4.0. Also for this sample it was concluded, based on IR photometry and monitoring, that it consists of long-period variable AGB stars (van der Veen & Habing 1990). Most of this sample has been observed in the OH(1612 MHz) maser line and about 70% of the sources were detected (te Lintel Hekkert et al. 1991), a much larger fraction than for the sample of Whitelock et al. The likely reason for the different OH detection rates is that the sample of van der Veen & Habing contains AGB stars surrounded by thicker shells.

The difference between both comparison samples is evident when we look at the distribution of the K-L colours and the pulsation periods (Figs. 5 & 6). The sample of van der Veen & Habing contains sources with significantly redder K-L colours and longer pulsation periods. Note that the periods of the van der Veen & Habing sample come from a paper in preparation and are not from the initial paper of 1990. It was shown by Whitelock et al. (1991) that in the initial paper of van der Veen & Habing

(1990) the periods longer than 1000 days were erroneous and these have been corrected now.

In Figs. 5 and 6 the distribution of K-L colours and pulsation periods for our sample of GC OH/IR stars is compared with those of the two comparison samples. It is clear that the distributions are very similar to the ones found by van der Veen & Habing (1990, 1997) and clearly shifted towards redder K-L colours and longer pulsation periods compared to the ones found for the Whitelock et al. sample. We thus conclude that the GC OH/IR stars appear similar to the reddest AGB stars such as the ones observed by van der Veen & Habing (1990).

In Fig. 5 we also show the distribution of periods for an OH selected sample of OH/IR stars in the galactic disk (Herman et al. 1984, Van Langevelde et al. 1990). It is very clear that this distribution spans a large range of periods from 200 to 2200 days, much wider than is found for the two sample of AGB stars in the bulge and our sample of GC OH/IR stars. However, when comparing these distributions one should keep in mind the strong selection effects present in the different samples. The period distribution of disk OH/IR stars extends towards shorter periods because the sample also contains nearby optical Miras with $P < 300$ days which have weaker OH emission than longer period OH/IR stars. This type of objects are unlikely to be found in our GC sample as VJGHW selected the brightest OH masers and very few foreground stars are expected. There also exists a bias towards longer periods for the disk stars as the longer period OH/IR stars tend to have higher OH maser luminosities and so for them the largest space volume is sampled. Although a similar selection effect is present for the sample of the GC OH/IR stars, where VJGHW selected the brightest OH masers for the variability study, the bias towards longer periods must be less because they are all at the same distance. There is no hard evidence that OH/IR stars with periods longer than 1000 days exist in the galactic centre region. There are however four OH/IR stars that may have periods between 1000 and 2000 days, but these periods could not be determined unambiguously (dashed line in Fig. 5), probably because the sources were monitored over a time interval of only about 1000 days. Because of these selection effects it remains somewhat unclear whether the apparent absence of GC OH/IR stars with periods longer than 1000 days is real.

A direct comparison of the bolometric magnitudes is more difficult because other samples have uncertain distances. Assuming that all objects in our sample are indeed at the same distance, a considerable spread in bolometric magnitudes is present even for sources for which good luminosity determinations are available (-6.5 $\lesssim M_{\rm bol} \lesssim$ -4.0; see Fig. 7). This spread is certainly larger than can be expected from the uncertainties in the measurements ($\lesssim$0.3 mag) and suggests a range of progenitor masses (1 to 3 $M_\odot$) and a range of ages (1 - 10 Gyr, Bertelli et al. 1994). We also note that the current luminosities exceed the preliminary ones found by Haller and Rieke (1989) in a search for galactic centre Miras. They find -on the basis of K magnitudes- a luminosity distribution which cuts off at $M_{\rm bol} \approx -4.5$ mag.

A difference exists between the GC OH/IR stars and the bulge IRAS sources. Van der Veen and Habing (1990) argue that

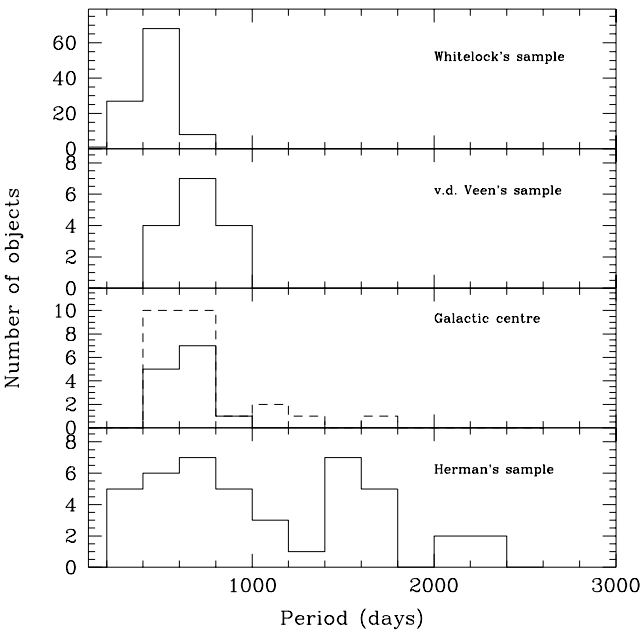

Fig. 5. Period distributions for different samples of long-period variable stars in our Galaxy; from top to bottom: a sample of IRAS sources in the bulge (Whitelock et al. 1991); the periods determined by van der Veen and Habing (1997) for a 'redder' IRAS sample in the bulge. The next panel shows the results of the sample under study (VJGHW). The dashed line denotes sources to which no unambiguous period could be attributed. The lowest panel shows the period distribution of stars in the disk (Herman et al. 1984, Van Langevelde et al. 1990).

all bulge stars may have luminosities between 5000 and 5500 $L_\odot$ (see also next section), so that the GC has an excess of higher luminosity stars. An excess of high luminosity stars relative to the luminosity function observed in the Baade window has been observed before (Lebofsky & Rieke, 1987, Rieke 1987 and 1993, Haller & Rieke 1989, Haller 1992, Sellgren et al. 1996). However and again, the GC sample does not have the OH/IR stars with the highest luminosity that are found in the galactic disk (e.g. van Langevelde et al. 1990 and Blommaert et al. 1994).

4.2. Kinematic populations

Lindqvist et al. (1992b) showed that within the original sample of 134 stars statistically significant kinematic differences are seen when the OH/IR stars are divided into two groups based on the expansion velocities of their shells (the separation between the blue and red-shifted peaks in the OH spectrum). That different expansion velocities trace different populations of OH/IR stars was found earlier (e.g., Baud et al. 1981). The high expansion velocities generally trace more luminous, and hence one assumes, more massive and thus younger OH/IR stars. One should realize that the age difference between low mass (1-2 $M_\odot$, a few 10^9 yrs) and high mass (6 $M_\odot$, a few 10^8 yrs) OH/IR stars is more than an order of magnitude.

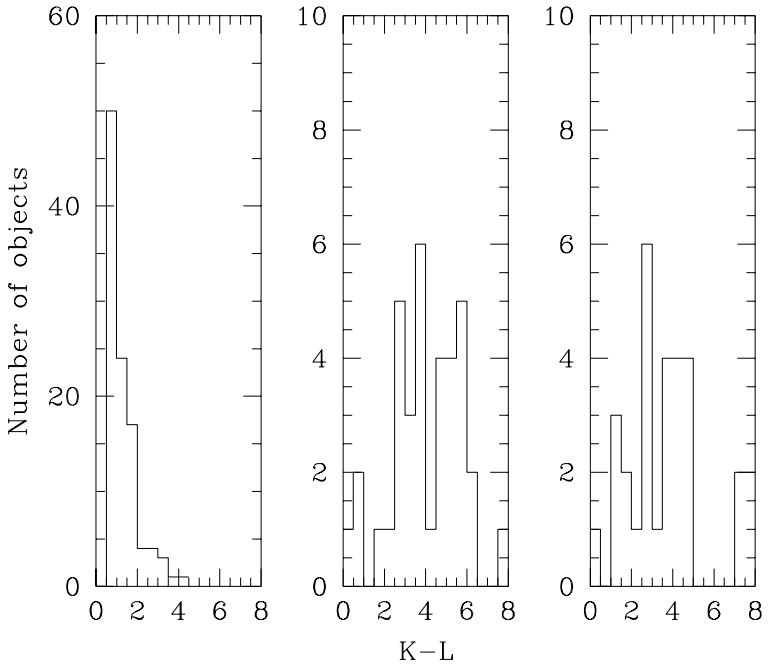

Fig. 6. K-L colour histograms for different samples of long-period variable stars. Left panel shows data by Whitelock et al. (1991) for a sample of IRAS sources in the bulge, centre panel: bulge OH/IR stars by van der Veen and Habing (1990), right panel: the current sample, extinction corrected.

Fig. 8 shows the histograms of the mean $M_{\rm bol}$ for the smaller expansion velocity group ($v_{\rm exp} < 18$ km/s) and the high expansion velocity stars ($v_{\rm exp} > 18$ km/s). We expect to see some of the kinematic difference in the luminosity distribution of these objects. It is clear that the small number of sources inhibits a firm conclusion. However, we indicate here some possible differences. The smaller expansion velocity group has an average value of $<$M$_{\rm bol}$ $>$ of -4.4. This is about the same value as was found by van der Veen and Habing (1990) ($5500L_{\odot}$ or $M_{\rm bol} = -4.5$). Suggesting that this subgroup may be related to the OH/IR star population of the bulge. Also the expansion velocities here have the same range as what is found in the bulge ($v_{\rm exp} < 17$ km/s, van der Veen and Habing 1990). The high expansion velocity stars, with a flatter kinematical distribution, have a broader luminosity distribution. It contains objects with the same luminosities as the smaller expansion group but almost half of its group has higher luminosities (M$_{\rm bol}$ < -5). This latter, "disk-like" population thus contains a large spread in ages (see previous section).

To further analyse the possible relationship of the galactic centre stars with the OH/IR stars in the bulge and the disk we take a look at the number densities. In Blommaert (1992) the surface distribution of red IRAS sources in the bulge is derived as function of latitude. On the basis of these calculations we expect to find 134 stars per square degree at the centre of the bulge. This happens to be the exact number of OH sources found by Lindqvist et al. in 6 VLA primary beam fields (in total ≈ 1 square degree), but is somewhat fortuitous. First, not all the red IRAS sources have OH masers; from van der Veen and Habing (1990) we learn that only 70% have OH maser emission. Although sources may be more efficient in masering the OH near the galactic centre (where more UV photons are available leading to a higher OH abundance) we still expect a contribution of similar sources without OH maser. Second, the Lindqvist et al. (1992a) sample of OH sources in the galactic centre is incomplete. Sjouwerman et al. (1996) show that with a more sensitive search 50% more objects are found. This means that about half of the OH/IR stars in the galactic centre can be considered as bulge stars ((70% of 134 expected)/134×1.5 found). This would agree with our suggestion that the low expansion velocity stars (half of the total sample) can be considered as bulge objects. The connection with the exponential disk is more complicated. On basis of modeling of the distribution of OH/IR stars detected in an IRAS based survey (te Lintel Hekkert et al. 1991) by Dejonghe (1992) one expects to find about 100 objects at the centre of the Galaxy. Blommaert et al. (1994) however, using a VLA survey along the galactic plane, show that a simple continuation of the exponential disk as observed at longer longitude and higher latitude is not likely as the number of OH/IR stars drops rapidly for $l \leq 10^{\circ}$. This decrease in the number of stars has also been seen in other surveys (Ng et al. 1996 and Paczynski et al. 1994). It thus seems unlikely that the disk-like distribution for the GC OH/IR stars is connected with the old stellar disk. Furthermore Catchpole et al. (1990) find in their near-infrared survey of the galactic centre an excess of stars with higher K luminosities which according to their model can only be attributed for a small part to the disk. The high luminosity objects are then to be considered as a population intrinsic to the galactic centre.

The expansion velocity of the circumstellar shell depends on both luminosity and metallicity (Schutte and Thielens, 1989 and Habing et al. 1994). The high expansion velocity group is really extreme because the luminosities are moderate with respect to those of disk OH/IR stars (previous section), nevertheless no other OH/IR stars in our Galaxy are known with expansion velocities as high. This indicates that the metallicities of this group

must be very high as we explain below. Although the luminosities are different for the two groups in our sample, this cannot explain the difference in expansion velocity. It would then follow that the metallicity is the main reason for the difference in the expansion velocities. This would be reflected in the ratio of the gas- ($\dot{M}_{\rm g}$) and dust-mass loss ($\dot{M}_{\rm d}$),

$$\mu = \dot{M}_{\rm g}/\dot{M}_{\rm d} \propto L_*^{0.5}\ v_{\rm exp}^{-2}, \qquad (2)$$

which is believed to depend on metallicity (van der Veen 1989). The $\langle L_*^{0.5}\ v_{\rm exp}^{-2}\rangle$ of the high expansion velocity group is only half as high as that of the low expansion velocity group (0.21 ($\pm$0.05) against 0.38 ($\pm$0.10)) indicating that the kinematically more "flattened" group is more metal-rich than the low expansion velocity group.

4.3. High-velocity stars

Van Langevelde et al. (1992a) made a small survey in the OH (1612 MHz) to search for OH/IR stars at high radial velocities in the galactic centre. They found two objects at absolute radial velocities larger than 300 km/s. We have observed these two objects in the infrared together with one star from an older survey (Baud et al. 1975) which also has a high radial velocity (-342 km/s). The two objects found by van Langevelde et al. (1992a) were detected and their bolometric magnitudes are included in Table 5. For the other star: OH0.334-0.181 no clear counterpart was found in the infrared (see Sect. 3.3.1). Van Langevelde et al. (1992a) discuss the nature of these stars which in the (l,v) diagram stand out clearly in comparison with the Lindqvist et al. sample. They conclude that these stars are most likely bulge objects on elongated orbits passing close to the galactic centre. The bolometric magnitudes we derived for these stars are -4.6 and -5.2 for OH359.837+0.120 and OH359.918-0.056 respectively. These bolometric magnitudes have not been corrected for variability as this information is not available. Van der Veen and Habing (1990) find an average bolometric magnitude of -4.5 for OH/IR stars in the bulge. Considering the amplitude of 1 magnitude in the average bolometric magnitude, we conclude that the observed luminosities do not contradict the conclusion of Van Langevelde et al. (1992a) that these sources are bulge stars.

4.4. Non-variable OH sources

In VJGHW a group of 11 OH masering sources was discussed for which no periods could be fitted (group 3). Seven of these sources were searched for in the infrared and four turned out to be peculiar. For OH359.952-0.036 and OH0.319-0.040 no counterpart was found in the centre of the IRCAM K- and nbL-images. A further search in J and H with IRCAM was also unsuccessful and around the central position only blue sources were found. Attempts to detect OH359.952-0.036 at 10 and 20 μm failed. Also OH359.755+0.155 was observed with IRCAM in the H, K and nbL band and we found a blue source near the centre of the image. The measurements in 1991 and 1993 in K and nbL only showed small variations. With UKT8 however a red source

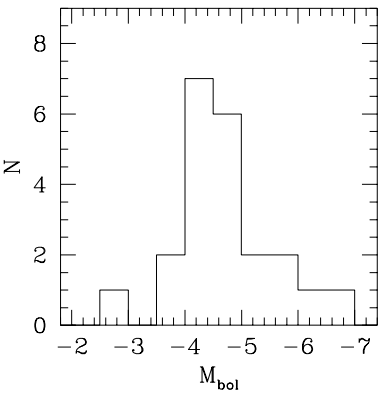

Fig. 7. Distribution of the average bolometric magnitudes of galactic centre OH/IR stars (only sources for which a variability correction was possible are included).

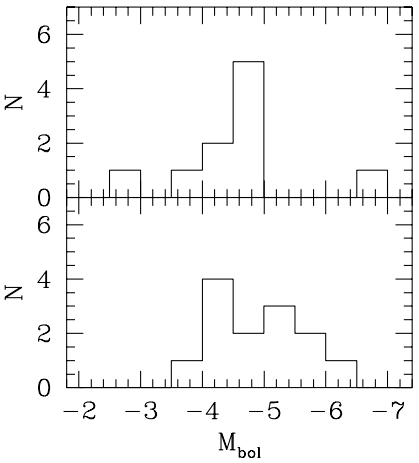

Fig. 8. Distributions of the average bolometric magnitudes of galactic centre OH/IR stars with $v_{\rm exp} < 18$ km/s (upper diagram) and those with $v_{\rm exp} > 18$ km/s (lower diagram). Only sources for which a variability correction was possible are included.

was picked up in the L′-band (3.8μm) (L′ − M = 0.67) for which it is not clear whether it is associated with the source found in the IRCAM image (IRCAM(K) − L′ = −0.12). For OH359.938-0.077 no counterpart was found in the K- and nbL-IRCAM images. The source was however detected around 10 μm and showed a silicate feature in absorption. As we were not able to find the source when searching in the L-band we tried to do aperture photometry in L and M simply by starting to integrate on the source position (relying on the accurate VLA position). It resulted in the lowest L- and M-band fluxes of the entire sample (Table 2). These four sources have OH "light curves" that show no sign of variability, although the maser is among the strongest masers of the sample.

For the three remaining sources, OH0.079-0.114, OH0.040-0.056 and OH0.225-0.055, infrared counterparts were found with colours comparable to the rest of the sample of OH/IR stars. These objects may have variable OH fluxes, but were too weak so that no clear period could be fitted. In fact the first two

sources were monitored by Jones et al. 1994 who find periods for these stars (700 and 670 respectively). These objects therefore seem to be normal pulsating OH/IR stars for which the period of regular variation in OH, however, could not be detected.

So, in contrast to the variable OH/IR stars for which in almost all cases a red counterpart was found, this seems not to be the case for the non-variable sources. Herman et al. (1984) were also unable to detect their non-variable OH sources in the infrared. Furthermore the angular sizes of the OH shells of these objects are very small and it was concluded that the non-variable stars either have small OH shells or are at very large distances. Van der Veen et al. (1989) suggest that the non-variable sources (see also Van Langevelde et al. 1990) are extremely red, which is certainly the case for OH359.938-0.077 which was only detected at longer wavelengths. The non-variable sources can then be linked to OH/IR stars with detached shells (Lewis 1989, Bedijn 1987): when the stellar envelope mass decreases below roughly 0.01 $M_\odot$ the surface temperature becomes very sensitive to the envelope mass (Schönberner 1983). When the envelope decreases further by hydrogen shell burning and/or mass loss the stellar surface becomes increasingly hotter. van der Veen et al. (1989) suggest that around this time the stellar pulsation stops and the mass loss drops significantly, leading to a dust shell that expands away from the star, dilutes and cools. In the end an increasingly hotter central star appears, resulting in the formation of a planetary nebula. The fraction of non-variable sources in our sample ($\sim$ 12.5%) is the same as the ratio of OH masering "early" planetary nebulae over OH/IR stars in the bulge (Zijlstra et al. 1989) ($\sim$ 13%). A problem with this interpretation is the fact that no counterparts were found in the shortest wavelengths which one expects as these sources become visible again. This could however, be explained by the fact that the extinction in the shortest wavelengths is very high and the fact that it is more difficult to distinguish a "bluer" source amongst field stars (in comparison to the red OH/IR stars in the rest of the sample).

Another type of objects which also fits the characteristics of the non-variable OH sources is that of the core helium burning supergiants. They turn up as very red objects (Wood et al. 1992) but are often still optically detectable. They are variable with very small amplitudes ($\sim$ 0.1 mag, whereas an OH/IR star typically has an amplitude of around 1 magnitude) and periods of several years. Wood et al. (1992) conclude that in their sample of IRAS sources in the Magellanic Clouds the reddest sources with no or only small amplitude variability are a mixture of post-AGB stars and supergiants. They make a distinction simply on the basis of the luminosity, which is above the AGB limit ($M_{bol} \sim -7.2$ mag) for the supergiants. As we do not have reliable luminosities for these OH sources we cannot make this distinction. That such high luminosity supergiants in the galactic centre may exist has also been suggested by Haller and Rieke (1989) and has been seen as evidence for recent star formation (less than 10^8 years ago) in the galactic centre.

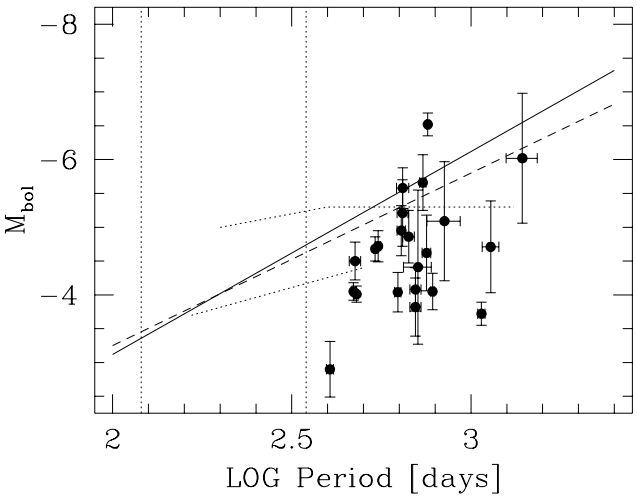

Fig. 9. $P - M_{bol}$ diagram for the galactic centre OH/IR stars. The error bars indicate 1σ-errors in M_{bol} and P. The dashed line is the PL relation by Whitelock et al. (1991), the solid line is by Feast et al. (1989). The vertical dotted lines indicate the range of periods of the LMC Miras (Feast et al. 1989). For comparison with our data points the evolutionary tracks for a 1 (lower track) and $2.5M_\odot$ (upper track) variable AGB star have been drawn (Vassiliadis and Wood (1993)).

4.5. The period-luminosity relation

The period-luminosity (PL) diagram for our sample of GC OH/IR stars is shown in Fig. 9. As mentioned earlier, we assume that all OH/IR stars are at the same galacto-centric distance of R_0 = 8 kpc. The error bars indicate 1σ-errors in M_{bol} and P.

For comparison we have drawn the PL relation by Feast et al. (1989) (solid line) and Whitelock et al. (1991) (dashed line). The linear relation derived by Feast et al. here after referred to as the *Mira* PL relation, is based on a sample of LMC Miras with periods shorter than 420 days. The observed rms scatter around this linear relation is only about 0.16 mag. The linear relation derived by Whitelock et al. hereafter referred to as the *modified* PL relation, is based on the combined samples of LMC Miras used by Feast et al. and galactic disk OH/IR stars with phase-lag distances (van Langevelde et al. 1990). Whitelock et al. argue that "the data seem consistent with the idea that the OH/IR stars fall on the extension of the PL relation to longer periods and higher luminosities" but that "more accurate distances are necessary to state this with certainty". Indeed, the galactic disk OH/IR stars have rather larger errors in their M_{bol} mostly due to uncertainties in the phase-lag distances of 20-50%.

We like to note that determining distances to individual disk stars with an accuracy of 20-50% is by itself very impressive and illustrates the usefulness of the phase-lag method. However, including other uncertainties this still results in an uncertainty in M_{bol} between 0.5 and 1.0 mag which is simply too large for the purpose of studying their location in the PL-diagram.

In Fig. 9 we present our sample of GC OH/IR stars for which the distance (i.e. the distance to the galactic centre) is well known. We have carefully calculated the combined error

due to uncertainties in the photometry, extinction correction and variability correction (see Sect. 3).

Given the location of the data points relative to the two PL relations and given the size of the error-bars two things are immediately clear. First, the galactic centre OH/IR stars are not on the extension of the *Mira* PL relation (solid line) and are not fitted by the *modified* PL relation (dashed line). In fact most points are systematically below both PL relations. Second, the spread in $M_{\rm bol}$ is large compared to the error-bars in $M_{\rm bol}$ which argues against the existence of a unique and linear PL relation for these stars. Of the 22 OH/IR stars plotted in Fig. 9 only seven (32%) are within one sigma of the LMC *Mira* PL relation (Feast et al.). One source (OH359.762+0.120; see Sect. 4.5.1) is significantly above the PL relation ($\sim 4\sigma$) and fourteen sources are more than 1σ below the PL relation.

Can this distribution in Fig. 9 be explained by possible systematic errors not taken into account in calculating the error bars? The only two sources of systematic errors that we could identify are those in the distance to the GC and the extinction correction. If we assume a distance of 9 kpc instead of 8 kpc all points in Fig. 9 move upwards by 0.26 mag and this does not make a significant change. The extinction correction contains two sources of possible systematic error: the used extinction curve and the value of $A_{\rm V}$. If, for given $A_{\rm V}$, we use the extinction curve by Rieke & Lebofsky (1985) instead of the curve by van de Hulst (1949) (see also the discussion in Sect. 3.1) all points in Fig. 9 move down by 0.15 mag to fainter $M_{\rm bol}$, against what we need. If we increase $A_{\rm V}$ the points in Fig. 9 move up by about 0.03 mag for each magnitude increase of $A_{\rm V}$. We have to increase $A_{\rm V}$ to more than 60 mag for the data points in Fig. 9 to spread evenly around the *Mira* PL relation. We reject this possibility as unrealistic. Patches of clouds of such high extinction towards the galactic centre do exist but certainly don't have an impact on the whole sample but at most at a few individual cases (see also Sect. 3.1). *We conclude that the data points for the GC OH/IR stars are significantly and systematically below the extension of the Mira PL relation.*

Deviations from the LMC *Mira* PL relation have been found before. Hughes & Wood (1990) studied a sample of optically identified Long Period Variables in the LMC which are similar to galactic Miras. They found that for periods below 300 days these objects follow the *Mira* PL relation well, but for longer periods the relation seems to bend upwards to higher $M_{\rm bol}$ at a given period than predicted by the *Mira* PL relation. For periods between 500 and 800 days the values for $M_{\rm bol}$ range between -5 and -7. Another sample of IRAS selected Long Period Variables in the LMC with faint or no optical counterparts and some with OH maser emission are found to be systematically above the *Mira* PL (Wood et al. 1992). They all have periods above 1000 days and $M_{\rm bol}$ between -6 and -7.5 but without an obvious relation between period and $M_{\rm bol}$. Finally Jones et al. (1994) found a result similar to ours for a sample of 15 GC OH/IR stars. There is a small overlap between our samples. Jones et al. finds periods between 400 and 1000 days and $M_{\rm bol}$ (with one exception) between -4 and -6 with no apparent correlation between $M_{\rm bol}$ and period. From the above data and the data presented in this paper it appears that no well defined PL relation exists for periods longer than about 500 days, whereas for periods below 300 days such a relation is well established (Feast et al. 1989).

In the literature of the past 10-15 years there have been two competing views on the interpretation of the PL diagram. One view is that a unique (and linear) PL relation outlines a mass sequence with the more massive stars having longer periods and more negative $M_{\rm bol}$ (Feast & Whitelock 1987, Whitelock 1995). An opposite view is that the PL diagram consists of evolutionary sequences along which short period Miras evolve into long period OH/IR stars (e.g. van der Veen 1989, Bedijn 1987). Support of the first idea is that kinematic data indicate that Miras of different periods belong to different population (Feast 1963). This argues against the interpretation of the PL relation as an evolutionary sequence in the sense that apparently not all stars evolve from the shortest to the longest period. In addition, the Mira phase is probably only $5\,10^4$ to $3\,10^5$ yr long. The increase of 1 mag per 10^6 yr is very modest.

We believe that these arguments are correct. However, we do not believe that a unique (linear) PL relation exists for all AGB stars and we do believe that, despite what is said above, evolutionary effects play a considerable role in the PL diagram. We agree with the interpretation of Jones et al. (1994) that the *Mira* PL relation represents the early parts of the evolutionary tracks of AGB stars with increasing main sequence progenitor masses stacked on top of each other. The GC OH/IR stars have evolved off the *Mira* PL relation towards longer pulsation periods because their increased mass loss has caused a significant decrease in stellar mass and therefore a significant increase in pulsation period. We will discuss this in a little more detail.

In Fig. 9 we have indicated model evolutionary tracks for $1M_{\odot}$ and $2.5M_{\odot}$ stars from Vassiliadis and Wood (1993) that illustrate the evolution off the *Mira* PL relation because of mass loss. The tracks are the result of the changes in both $M_{\rm bol}$ and P. The change in $M_{\rm bol}$ is caused by the growth of the hydrogen exhausted core due to hydrogen shell burning. The rate of change is constant at about -0.08 mag per 10^5 yr (Wood, 1990). The change in $\log P$ follows from classical pulsation theory which states that $P \sim R^a\, M^{-b},\ (a > 0, b > 0)$. When a star ascends the AGB its radius increases, due to the increase in luminosity and the decrease in surface temperature, and its mass decreases due to mass loss. Using Wood (1990) the result is an increase in $\log P$ at a constant rate of 0.05 per 10^5 yr due to its increasing luminosity and an additional $0.67 \int_0^{10^5} \dot{M} dt = 0.67\, M_{lost}$ due to mass loss, where M_{lost} is the total mass lost in 10^5 years.

In this interpretation the spread of points to one side of the *Mira* PL relation is due to evolution as the evolutionary tracks have slopes much flatter (between -1.57 and 0 depending on the mass loss rate) than the slope of the *Mira* PL relation (-3.3 according to Feast et al. 1989). This implies that the *Mira* PL relation roughly represents the begin points of the evolutionary tracks for stars with different initial masses with the more massive stars starting their evolutionary track at longer pulsation periods and higher luminosities. We use the word 'roughly' because the actual starting points of the evolutionary tracks (given

their flat slopes) would likely be to the left of the *Mira* PL relation as shown in Fig. 9.

Our observations of the GC OH/IR stars support this view of evolution off the *Mira* PL relation towards longer periods. However, it also shows a problem with the model of Vassiliadis and Wood (1993). The evolutionary tracks for stars with less than $1.5M_{\odot}$ do not extend far enough to the right towards longer periods. At a maximum $M_{\rm bol}$ of -4.5 these stars would reach a maximum period of only 630 days according to Vassiliadis & Wood (1993) where we find five stars with periods between 700 and 1000 days and $M_{\rm bol} > -4.5$.

In conclusion, we believe that our observations in combination with other data discussed at the beginning of this section supports the following interpretation of the PL diagram. Depending on the initial progenitor mass stars start to pulsate with a period that depends on their initial mass. The higher the initial progenitor mass the longer the pulsation period and the higher their luminosity. These starting points form a rather well defined sequence in the PL diagram somewhat to the left of the observed *Mira* PL relation. The observed *Mira* PL relation represents the average position of Miras with more massive Miras located at higher pulsation periods and higher luminosities. The *Mira* PL relation is therefore mostly a mass sequence although evolutionary effects which effectively broaden the relation are present. This part of the interpretation is in agreement with the interpretation given by Feast et al. (1989) and Whitelock et al. (1991). It also explains the kinematic differences between Miras with different pulsation periods. We differ, however, significantly from the interpretation by Feast et al. and Whitelock et al. in the second part of the interpretation. We conclude that once the mass loss increases and the stars become OH/IR stars their pulsation periods increase and they move away from the LMC Mira PL relation towards longer periods. According to our data even stars with low luminosities ($M_{\rm bol}$ as low as -4) apparently do reach pulsation periods as long as 1000 days. This is not predicted by the model of Vassiliadis & Wood (1993) for which Miras with masses below $1.5M_{\odot}$ do not reach such long pulsation periods.

4.5.1. OH 359.762+0.120, a foreground source?

This source is quite exceptional. If it is at the galactic centre it is by far the brightest AGB star of the whole sample. It is also amongst the strongest OH emitters in the sample. The phase lag determined by VJGHW is 39.6 days (σ = 7.4 days) which is the largest value of the galactic centre sample. Could it be a foreground object? OH359.762+0.120 was first used by Van Langevelde & Diamond (1991) to map interstellar extinction and later by Frail et al. 1994 to study anisotropic scattering toward the Galactic centre. Both studies unambiguously show that this star must be behind the scattering medium. The study by Frail et al. 1994 seems to indicate that the screen is associated with the Galactic centre environment, more recently Lazio et al. 1995 arrive at similar conclusions. This makes the interpretation as a foreground object unlikely. If OH359.762+0.120 is really at the Galactic centre, its special place in the P-L diagram of the galactic centre stars (above the PL-relation in stead of on or below it, like the other stars in our sample) could be a clue of it being an object of a peculiar nature. One such interpretation was investigated in a recent paper by van Paradijs et al. 1995, but turned out to be inconclusive. On the other hand the high luminosity for this star, when at 8 kpc, does not exceed the AGB limit (contrary to what is indicated in Paradijs et al. 1995 who erroneously state a luminosity of $3 \times 10^5 L_{\odot}$ based on the results in this paper and Jones et al. 1994), so a rejection of a 8 kpc distance depends on the existence of a tight period-luminosity relation. In the previous section we questioned the existence of a PL-relation but for sources which fall below that relation and not above, however, as was already stated in Sect. 4.5, Wood et al. (1992) also find for the LMC OH maser sources that fall above the same relation. We conclude that independent research on the "scattering screen" towards the galactic centre indicates that this source is indeed situated in the centre of our Galaxy. Although its remarkable OH maser and infrared characteristics there is no clear evidence theat this object is not a genuine AGB-type OH/IR star.

5. Summary

We have shown that the mean colours, periods of a population of OH/IR stars in the galactic centre do not differ significantly from those found in a comparable sample of evolved stars in the galactic bulge. We also find a clear overlap in luminosities although the galactic centre does contain objects of higher luminosities which indicates more recent star formation. The low number of objects prohibits a firm conclusion on possible differences in luminosity between the two groups of stars divided on the basis of their expansion velocities. However, we find that the luminosities and the number density of low expansion velocity OH/IR stars in the galactic centre suggest that they are an extension of the bulge population. The high expansion velocity group contains stars with higher luminosities, is more metal-rich than the low expansion velocity group and is more likely a population intrinsic to the galactic centre.

We find that the OH/IR stars fall systematically below the period-luminosity relation proposed by Whitelock et al. (1991). The reason for this deviation may be the extreme mass loss that seriously affects the evolution of these OH/IR stars by increasing mostly the periods and by a lesser extend the luminosities. We rule out the possibility that the deviation from the Mira period-luminosity relation is the result of a bias in the determination of bolometric luminosities, although several difficulties were encountered in particular in the corrections for interstellar extinction.

Another interesting feature is the infrared peculiarity of the non-variable OH stars. For these objects only a weak or very blue near infrared counterpart was found. In the latter case the identification is uncertain and a weaker (red) counterpart may exist. We suggest that some of these objects are extremely red. Their properties suggest that the group consists of post-AGB stars and/or supergiants.

Acknowledgements. We thank Andrea Moneti at ESO and Tom Geballe, Tim Hawarden and Mark Casali at UKIRT for assistance with

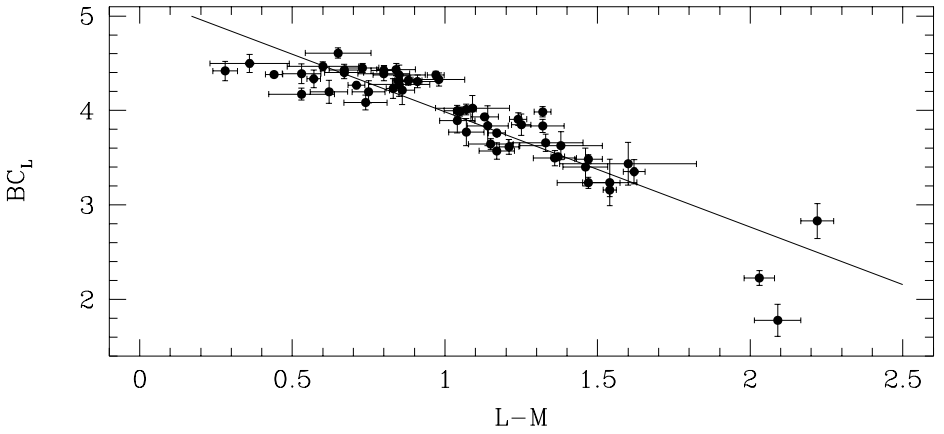

Fig. 10. The far infrared bolometric correction for OH/IR stars as a function of L - M colours, based on measurements of Blommaert et al. 1993 and by van der Veen and Habing (1990).

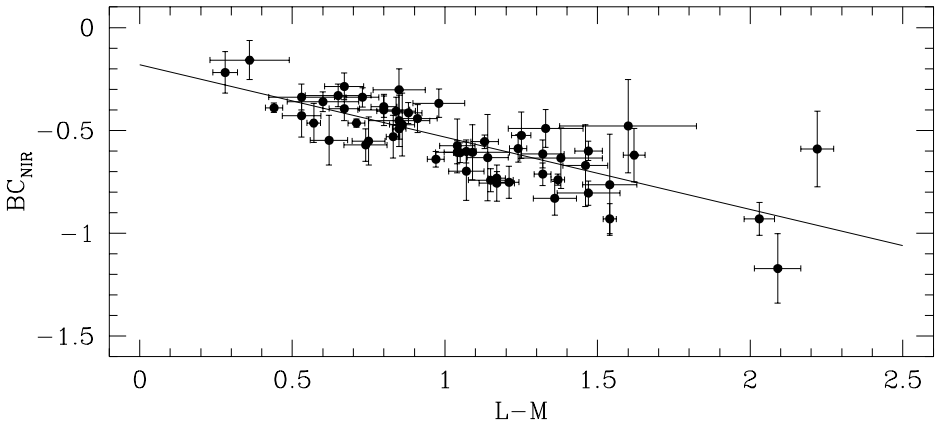

Fig. 11. The bolometric correction on the L-band magnitude for OH/IR stars as a function of L - M colours, based on measurements of Blommaert et al. 1993 and van der Veen and Habing (1990).

the observations and data reduction. We thank Nicolas Epchtein for his valuable input at the start of this project. The discussions with Ian Glass on the interstellar extinction, Yuen Ng on the galactic disc structure and with Maartje Sevenster on the dynamical point of view on the OH/IR star population(s) were very much appreciated. We thank the (anonymous) referee for his valuable suggestions. JB acknowledges support from the Netherlands Organisation for Scientific Research (NWO). HJvL acknowledges support for his research by the European Union under contract CHGECT920011.

Appendix A

We have determined two bolometric corrections to calculate $m_{\rm bol}$. We used samples of OH/IR stars in the galactic bulge (van der Veen and Habing 1990) and disk (Blommaert et al. 1993) for which near IR 2-12μm and IRAS 12-60μm photometry is available. Bolometric magnitudes were determined by integrating the SED between 2 and 60 μm. To account for the part shortward of 2 μm a black body was fitted to the blue part of the SED which was then integrated. To account for the part longward of 60μm it was represented by a λ^{-4} power law which was integrated between 60 and 200μm.

The integration was done by calculating F_ν as function of ν and applying the trapezium integrating rule by connecting the F_ν values by straight lines. By applying the trapezium rule to various black body curves and various compositions of two back body curves sampled at the same wavelengths or frequencies as our spectra we found that integration of F_ν over ν yields more accurate results than integration of F_λ over λ. We calculated both $m_{\rm bol}$ and $m_{\rm NIR}$ defined as the total flux between 2.2 (K-band) and 12.9μm (N3-band). It turns out that one has to apply only a small correction of 0.02 mag to the result of the trapezium rule integration to get the correct $m_{\rm bol}$ and a correction of +0.06 mag to get the correct m_{NIR} We now define two bolometric corrections: $m_{\rm bol} = m_{\rm NIR} + BC_{\rm NIR}$ and $m_{\rm bol} = L + BC_L$, where $\rm BC_L$ and $\rm BC_{NIR}$ are a function of L-M colour.

In Figs. 10 and 11 these bolometric corrections are plotted as function of L-M. Linear least square fits to the data points yield the following relations

$$BC_{NIR} = -0.18(\pm0.04) - 0.35(\pm0.04)(\mathrm{L-M}) \quad \text{(A1)}$$

$$BC_{\rm L} = 5.21(\pm0.08) - 1.22(\pm0.07)(\mathrm{L-M}) \quad \text{(A2)}$$

The least square fits gave correlation coefficients of 0.88 and 0.91 respectively.

References

Baud, B., Habing, H.J., Matthews, H.E., Winnberg, A., 1981, A&A 95, 156

Baud, B., Habing, H.J., Osullivan, J.D., Winnberg, A., Matthews, H.E.: 1975, Nature 258, 406
Becklin, E.E., Neugebauer, G.: 1968, ApJ 151, 145
Bedijn, P.J.: 1987, A&A 186, 136
Bertelli, G., Bressan, A., Chiosi, G., Fagotto, F., Nasi, E.: 1994, A&AS 105, 275
Blommaert, J.A.D.L., 1992, thesis, University of Leiden, The Netherlands (Chapter 2)
Blommaert, J.A.D.L., van der Veen, W.E.C.J., Habing, H.J.: 1993, A&A 267, 39
Blommaert, J.A.D.L., Van Langevelde, H.J., Michiels, W.F.P.: 1994, A&A 287, 479
Catchpole, R.M., Whitelock, P.A., Glass, I.S.: 1990, MNRAS 247, 479
Cohen, R.J.: 1989, *Rep. Prog. Phys.* 52, 881
Dejonghe, H.: 1992. In: Weinberger and Acker (eds.) Proc. IAU Symp. 155, Planetary Nebulae. Kluwer Academic Publishers, p. 541
Elitzur, M.: 1992, "Astrophysical Masers", Kluwer Academic Publishers, Dordrecht
Engels, D., Kreysa, E., Schultz, G.V., Sherwood, W.A.: 1983, A&A 124, 123
Feast, M.W.: 1963, MNRAS 125, 27
Feast, M.W., Glass, I.S., Whitelock, P.A., Catchpole, R.M.: 1989, MNRAS 241, 375
Feast, M.W., Whitelock, P.A.: 1987, in "Late Stages of Stellar Evolution", S. Kwok, S.R. Pottasch, eds., D. Reidel Publ. Cy, p.33
Frail, D.A., Diamond, P.J., Cordes, J.M., Van Langevelde, H.J.: 1994, ApJ 427, L43
Genzel, R., Hollenbach, D., Townes, C.H.: 1994, Rep. Prog. Phys. 57, 417
Glass, I.S., Matsumoto, S., Ono, T., Sekiguchi, K.: 1996, in "The Galactic Centre", Proceedings of 4th ESO/CTIO Workshop, R. Gredel, ed., Astr. Soc. Pac. Conf. Ser. 102, p. 312
Habing, H.J., 1996, A&A Review 7, No. 2
Habing, H.J., Tignon, J., Tielens, A.G.G.M.: 1994, A&A 286, 523
Haller, J.W.: 1992, Ph.D. Dissertation, University of Arizona, Tucson
Haller. J.W., Rieke, M.J.: 1989, in IAU Symposium No. 136: "The Centre of the Galaxy", ed. M. Morris (Kluwer Academic Publishers) p.487
Harvey, P.M., Bechis, K.P., Wilson, W.J., Ball, J.A.: 1974, ApJS 27, 331
Herman, J., Habing, H.J.: 1985, A&AS 59, 523
Herman, J., Isaacman, R., Sargent, A., Habing, H.J.: 1984, A&A 139, 171
Hughes, S.M.G., Wood, P.R.: 1990, AJ 99, 748
Jones, T.J., Hyland, A.R., Caswell, J.L., Gatley, I.: 1982, ApJ 253, 208
Jones, T.J., McGregor, P.J., Gehrz, R.D., Lawrence, G.F., 1994, AJ 107, 1111
Lazio, T., Joseph, W., Cordes, J.M., Frail, D.: 1995, BAAS 186, 50.04
Lebofsky, M.J., Rieke, G.H.: 1987, in "The Galactic Centre", AIP Conf. Proc. 155, p. 79, ed. Backer, D.C., American Inst. of Physics, New York.
Lewis, B.M.: 1989, ApJ 338, 234
Lindqvist, M., Habing H.J., Winnberg A.: 1992b, A&A 259, 118
Lindqvist, M., Winnberg A., Habing H.J., Matthews H.E.: 1992a, A&AS 92, 43
Ng, Y.K., Bertelli, G., Chiosi, C., Bressan, A.: 1996, A&A 310, 771
Okuda, H., Shibal, H., Kobayashi, Y., Kaifu, N., Nagata, T., Gatley, I., Geballe, T.R.: 1990, ApJ 351, 89
Paczynski, B., Stanek, K.Z., Udalski, A., Szymanski, M., Kaluzny, J., Kubiak, M., Mateo, M.: 1994, AJ 107, 2060
Reid, M.J.: 1993, ARAA 31, 345
Rieke, M.J.: 1987, in: "Nearly Normal Galaxies", Faber, S.M., ed., Springer-Verlag, New York, p. 90
Rieke, M.J.:1993, in "Back to the Galaxy", S. Holt and F. Verter, eds., (AIP Press: New York), p. 37
Rieke, G.H., Lebofsky, M.J.: 1985, ApJ 288, 618
Schönberner, D.: 1983, ApJ 272, 708
Schutte, W.A., Tielens, A.G.G.M.: 1989, ApJ 343, 369
Sellgren, K.: 1989, in IAU Symposium No. 136: "The Centre of the Galaxy", M. Morris, ed., Kluwer Academic Publishers, p.477
Sellgren, K., Blum, R.D., DePoy, D.L.: 1996, "The Galactic Centre", Proceedings of 4th ESO/CTIO Workshop, R. Gredel, ed., Astr. Soc. Pac. Conf. Ser. 102, p. 285
Sjouwerman, L., Winnberg, A., Van Langevelde, H.J., Habing, H.J., Linqvist, M.: 1996, "The Galactic Centre", Proceedings of 4th ESO/CTIO Workshop, R. Gredel, ed., Astr. Soc. Pac. Conf. Ser. 102, p. 294
te Lintel Hekkert, P., Caswell, J.L., Habing, H.J., Haynes, R.F., Norris, R.P., 1991, A&AS 90, 327
van de Hulst, H.C.: 1949, *Rech. Astr. Obs. Utrecht* Vol. 11. Part 2
van der Veen, W.E.C.J.: 1989, A&A 210, 127
van der Veen, W.E.C.J., Habing, H.J.: 1988, A&A 194, 125
van der Veen, W.E.C.J., Habing, H.J.: 1990, A&A 231, 404
van der Veen, W.E.C.J., Habing, H.J.: 1997, *in preparation*
van der Veen, W.E.C.J., Habing, H.J., Geballe, T.R.: 1989, A&A 226, 108
Van Langevelde, H.J., Brown, A.G.A., Lindqvist, M., Habing, H.J., de Zeeuw, P.T.: 1992a, A&A 261, L17
Van Langevelde, H.J., Diamond, P.J.: 1991, MNRAS, 249, *Short Communication*, 7P
Van Langevelde, H.J., Frail, D.A., Cordes, J.M., Diamond, P.J.: 1992b, ApJ, 396, 686
Van Langevelde, H.J., Janssens, M., Goss, M., Habing, H.J., Winnberg, A.: 1993, A&AS, 101, 109 (VJGHW)
Van Langevelde, H.J., Van der Heiden, R., Van Schooneveld, C.: 1990, A&A 239, 193
Van Paradijs, J., Spruit, H.C., Van Langevelde, H.J., Waters, L.B.F.M.: 1995, A&A 303, L25
Vassiliadis, E., Wood, P.R.: 1993, ApJ 413, 641
Whitelock, P.A., Feast, M.W., Catchpole, R.M.: 1991, MNRAS 248, 276
Whitelock, P.A.: 1995, Ap&SS 230, 177
Wood, P.R.: 1990, in "From Miras to Planetary Nebulae: Which Path for Stellar Evolution?", M.O. Mennessier & A. Omont, eds., Editions Frontières, Gif sur Yvette, p.67
Wood, P.R., Whiteoak, J.B., Hughes, S.M.G., Bessell, M.S., Gardner, F.F., Hyland, A.R.: 1992, ApJ 397, 552
Zijlstra, A.A., te Lintel Hekkert, P., Pottasch, S.R., Caswell, J.L., Ratag, M., Habing, H.J.: 1989, A&A 217, 157

This article was processed by the author using Springer-Verlag LaTeX A&A style file *L-AA* version 3.